11^{th} International Conference on Fracture Mechanics of Concrete and Concrete Structures
FraMCoS-11
J. M. Chandra Kishen, A. Ramaswamy, S. Ray and R. Vidyasagar (Eds)
https://doi.org/10.21012/FC11.092321

HOW DO CORROSION-DRIVEN MECHANISMS CHANGE CEMENTITIOUS MATERIAL'S PORE STRUCTURE AND IMPACT THE CORROSION-DRIVEN FRACTURE?

Mohit Pundir*, Ueli Angst*, and David S. Kammer*

*Institute for Building Materials, ETH Zurich
Zurich, Switzerland
e-mail: mpundir@ethz.ch

Key words: Cohesive Fracture, Fiber Reinforced Concrete, Composites, Durability

Abstract. Corrosion of reinforcement bars in concrete plays a significant role in determining a structure's durability and serviceability lifetime. Corrosive species diffuse through the pore space of cementitious material and chemically react to form corrosion products. These precipitates grow within the confined pores and exert pressure on the solid phase, which leads to fracture initiation and, ultimately, to a structure's deterioration. The deposition of corrosion products and internal cracking changes the pore structure over time, consequently influencing various mechanisms (ion diffusion, precipitate growth, stress development) that lead to corrosion-driven concrete fracture. In this contribution, we summarize how various processes change the pore structure of a cementitious material. We employ numerical simulations to analyze how different corrosion-driven processes, such as the deposition of corrosion products and the initiation and propagation of cracks, occur within a complex microstructure. We discuss how various corrosion-driven mechanisms lead to crack initiation and propagation at the microscale, changing microstructural details over time. Finally, we discuss how incorporating information about micro-structural details and their evolution may lead to better predictive models for corrosion-driven fracture.

1 INTRODUCTION

Corrosion of reinforcement bars in concrete plays a significant role in determining a structure's durability and, hence, its serviceability lifetime. Ferrous ions released at the steel-concrete interface diffuse through the pores and undergo many chemical reactions, forming rust (ferrous/ferric precipitates). A precipitate, confined in the pore space, grows with time, exerting pressure on the walls. Internal cracking begins when the surrounding matrix's stress exceeds the material strength. (see Figure 1). The three corrosion-driven mechanisms- ionic diffusion, chemical reactions, and stress development- co-occur at the micro-scale (within pores ranging from nanometers to micrometres) and subsequently influence the load-bearing capacity at the macro-scale. Thus, the pore structure and the pore space in cementitious material play a crucial role from the initiation of corrosion until the crack nucleation. The pore structure in concrete is highly complex, with pore sizes ranging from nanometers to micrometres, and this complexity of the micro-structure evolves due to the corrosion-driven mechanisms. The two main process that changes a micro-structure are micro-cracks formed due to the expansion of precipitates within the pores and pore-clogging due to the deposition of precipitates within the micro-pores. Since the corrosion-driven processes occur at a very small scale it

is difficult to observe these process experimentally. In the following section, we employ numerical methods to study the micro-structural changes at microscale. In particular, we look into the crack initiation and formation around the micro-pores.

2 MULTI-PHYSICAL PROCESSES IN FRACTAL MEDIA

In this paper, we employ spectral-based approach [1–3] to simulate the diffusion of ions and the development of stresses. Although the numerical methods used in the literature [4–11] have been crucial to the understanding of corrosion-driven damage, these methods (the Finite element method, the pore network model, and the Lattice Boltzmann method) approximate the real micro-structure in the cementitious material to reduce the high computational cost associated with the simulation of ion diffusion, stress development and crack initiation in a fractal domain. Applying the Fast-Fourier Transform (FFT) to solve partial differential equations in spectral methods makes the simulation of physical processes within a complex domain computationally efficient compared to other methods. Furthermore, an FFT-based approach requires a pixel-based representation of the structure; therefore, the approach can be employed to μ-CT scans of cementitious materials directly without making any approximations.

We consider a cementitious bar exposed to a constant flux of ferrous ions from one end. Each material point of the bar is coupled to a 2D representative volume element (RVE), shown in Figure 2a. We perform multi-scale simulations for the ionic diffusion of ferrous ions. At the macro-scale, we solve a transient diffusion equation (see Equation (1)). Within coupled RVEs, we solve a static diffusion equation until the average microscopic concentration gradient is equal to the macroscopic concentration gradient *i.e.* $\langle \nabla c(x) \rangle = \nabla c(X)$. Thus, the two equations for diffusion at two different scales are given as

$$\frac{\partial c(X)}{\partial t} + \nabla j(X) = f, \quad \nabla D \nabla c(x) = 0 \quad (1)$$

where D represents the intrinsic diffusion coefficient of ionic species. For this example, we consider a pore solution constantly buffered at a pH of 8 and the formation of ferrous hydroxide $Fe(OH)_2$ as the only corrosion product. The stress develops within the RVE due to the volumetric expansion of ferrous hydroxide, given as

$$\boldsymbol{\nabla} \underbrace{\mathbb{C} : (\boldsymbol{\varepsilon}(\boldsymbol{x}) - \boldsymbol{\varepsilon}_{\text{eig}}(\boldsymbol{x}))}_{\boldsymbol{\sigma}} = 0, \quad \ni \langle \boldsymbol{\varepsilon}(\boldsymbol{x}) \rangle = \mathbf{0} \quad (2)$$

where $\boldsymbol{\varepsilon}_{\text{eig}}(\boldsymbol{x})$ is the eigen strain developed due to the expansion of ferrous hydroxide at a microscopic point within pores of an RVE. We employ a phase-field approach [12] to simulate fracture initiation and propagation within an RVE.

$$-\frac{\mathcal{G}_c l_0}{2} \boldsymbol{\nabla} \cdot \boldsymbol{\nabla} d + \frac{\mathcal{G}_c}{2 l_0} d + \mathcal{H}^+ d = \mathcal{H}^+ \,. \quad (3)$$

Figure 2 shows the evolution of the pore network in the considered RVE due to micro-cracking. The precipitation of ferrous hydroxide leads to crack initiation and propagation within an RVE. We show how the precipitation occurs within the pores of the micro-structure, with maximum precipitation happening within the small pores. As these precipitates expand within the pore space, the surrounding solid matrix is damaged, leading to fracture initiation and propagation. As observed, the evolution of micro-cracks within the solid phase is complex. Due to the complex crack propagation, certain fragmented solid phases under pure compression inhibit crack growth, and therefore, the average RVE damage saturates around 0.35 Figure 3a. As a result, the total porosity of the considered RVE also saturates around 0.45. Interestingly, the total damage and the total porosity of the RVE never go to 100%, unlike what is assumed in several studies.

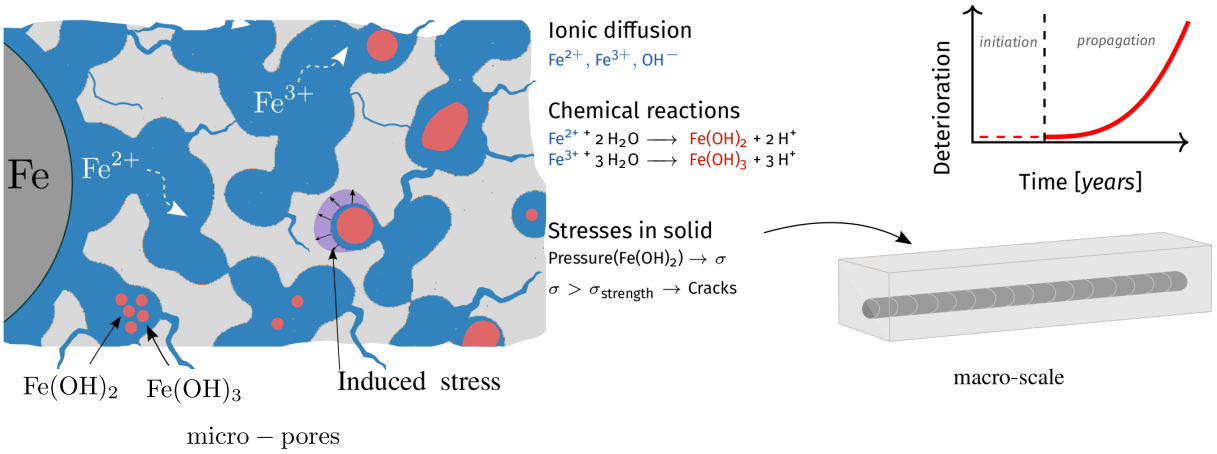

Figure 1: Schematic showing the different corrosion-driven mechanisms within micro-pores of concrete and the interplay among them that leads to corrosion-driven damage in concrete at structural scale.

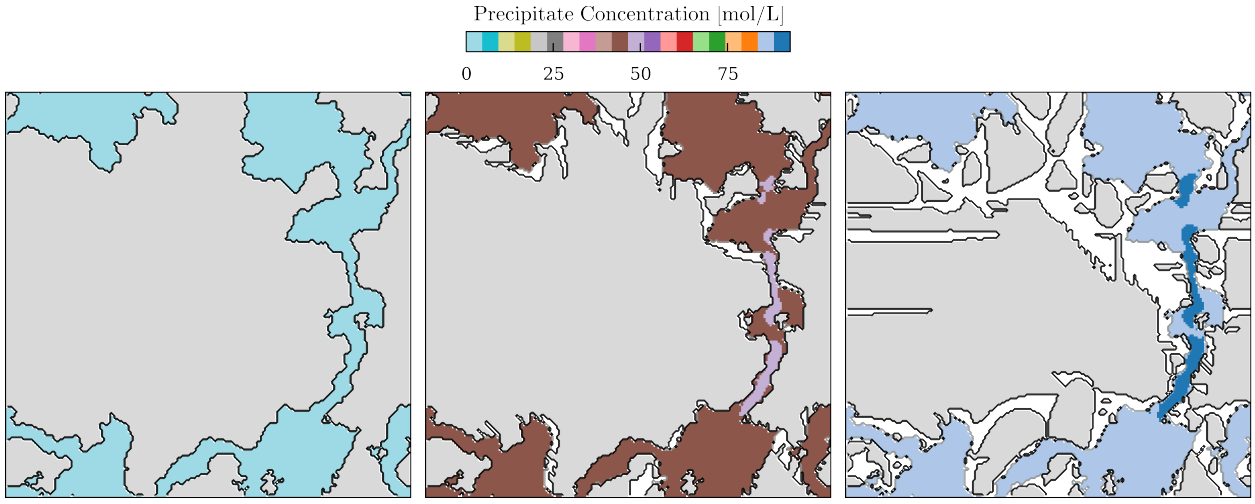

Figure 2: RVE Snapshots show the pore structure's evolution within the RVE due to micro-cracking. The leftmost figure shows the actual pore structure with the RVE before the start of the simulation. The precipitate concentration is zero everywhere within the pores. The middle figure shows the precipitation of ferrous hydroxide and the simultaneous initiation of cracks (shown in white) around the pores. The maximum precipitation occurs within the constricted portions of the pore network (as seen by the purple colour). The right-most figure shows the final state of the RVE and the new pore channels created due to the fracture propagation at time $t = 3500$ sec. We show micro-cracks (in white) only for damage values greater than 0.8.

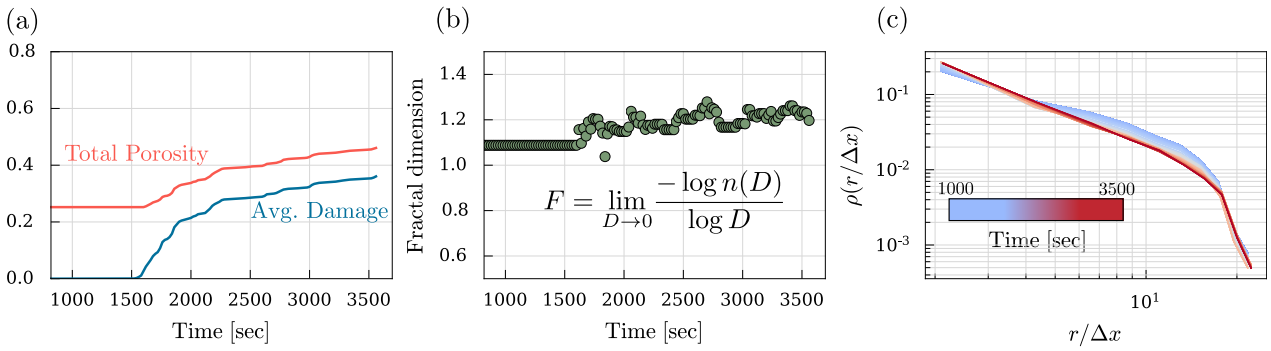

Figure 3: (a) Evolution of total porosity of the RVE (shown in red) and the average damage in the RVE (shown in blue). Both quantities saturate over time. The initial porosity of the RVE is 0.26. (b) The evolution of fractal dimension F for pore structure. The fractal dimension is computed from the box-counting method where D represents the box size and $n(D)$ is the number of boxes of size D that could fit within the pore space. (c) The radial density function and its evolution over time. The radial density function is computed from the distance transform of pore space.

3 CHARCTERIZATION OF FRACTURED MICROSTRUCTURE

In this section, we characterize the fractured micro-structure. Various measures exist in the literature to describe a porous micro-structure, namely, pore size distribution, $n-$point correlation function, and fractal dimension [13–20]. For this example, we mainly chose two measures: fractal dimension, which gives an estimate of the roughness of the pore walls, and radial density function, which provides an estimate of the pore size distribution [21]. Figure 3b-c shows the evolution of these two measures for the evolving RVE. The fractal dimension of the pore network increases from an initial value of 1.1 to 1.2. As the propagation and initiation of new cracks within the solid phases stop (as shown by the saturated value of the average damage in Figure 3a), the evolution of the fractal dimension also saturates to roughly 1.2. We also analyze the distribution of radial density function within the pore network. This measure, as defined by Torquato [21], gives the probability of finding a point at a radial distance between r and dr from the solid interface. Compared to other measurements (such as Mercury-Intrusion-Porosimetry (MIP), NAD), the radial density function gives a better estimate of pore size distribution since it does not assume the pore shape to be spherical or cylindrical. Similar to the fractal dimension, the radial density function also saturates. We see that the initiation of micro-cracks mostly leads to the creation of smaller pores as seen by the increase in probability density of smaller pores ($(r/\Delta x < 0.4)$ and decrease in the density of bigger pores ($r/\Delta x > 0.4$).

In this study, we did not consider the pore structure changes due to the deposition of the ferrous hydroxide. However, in reality, the precipitation should lead to clogging of pore space, especially small pores, as seen in Figure 2b-c. This should decrease the total porosity and, therefore, is expected to affect how cracks initiate and propagate within the solid material. Both phenomenons *i.e.* crack initiation and pore-clogging must be considered simultaneously to fully understand the pore structure evolution during corrosion-driven damage in concrete. Finally, we believe that the characteristics measures that represent evolution of micro-structure must be taken into consideration for predicting deterioration of structures sue to corrosion-driven process.

4 CONCLUSIONS

In this paper, we employ a spectral-based method to numerically simulate a corrosion-driven process within an actual micro-structure of cementitious material. We show how precipitation of corrosion products leads to the initiation and propagation of micro-cracks and how this changes the pore structure over time. Due to the complexity of the crack network, a micro-

structure is never damaged completely. The total damage within a micro-structure naturally depends on the initial micro-structure and its evolution. We characterize the evolving structure, which shows that the pore structure's evolution saturates and reaches a steady state. We believe that micro-structure evolution should be considered within the predictive models.

REFERENCES

[1] H. Moulinec and P. Suquet, "A numerical method for computing the overall response of nonlinear composites with complex microstructure," *Computer Methods in Applied Mechanics and Engineering*, vol. 157, pp. 69–94, Apr. 1998.

[2] T. W. J. de Geus, J. Vondřejc, J. Zeman, R. H. J. Peerlings, and M. G. D. Geers, "Finite strain FFT-based non-linear solvers made simple," *Computer Methods in Applied Mechanics and Engineering*, vol. 318, pp. 412–430, May 2017.

[3] R. J. Leute, M. Ladecký, A. Falsafi, I. Jödicke, I. Pultarová, J. Zeman, T. Junge, and L. Pastewka, "Elimination of ringing artifacts by finite-element projection in FFT-based homogenization," *Journal of Computational Physics*, vol. 453, p. 110931, Mar. 2022. arXiv: 2105.03297.

[4] B. Šavija, M. Luković, J. Pacheco, and E. Schlangen, "Cracking of the concrete cover due to reinforcement corrosion: A two-dimensional lattice model study," *Construction and Building Materials*, vol. 44, pp. 626–638, July 2013. Publisher: Elsevier.

[5] K. Bhargava, A. K. Ghosh, Y. Mori, and S. Ramanujam, "Modeling of time to corrosion-induced cover cracking in reinforced concrete structures," *Cement and Concrete Research*, vol. 35, pp. 2203–2218, Nov. 2005. Publisher: Pergamon.

[6] S. Guzmán and J. C. Gálvez, "Modelling of concrete cover cracking due to non-uniform corrosion of reinforcing steel," *Construction and Building Materials*, vol. 155, pp. 1063–1071, Nov. 2017. Publisher: Elsevier Ltd.

[7] C. Cao and M. M. Cheung, "Non-uniform rust expansion for chloride-induced pitting corrosion in RC structures," *Construction and Building Materials*, vol. 51, pp. 75–81, Jan. 2014. Publisher: Elsevier.

[8] P. F. Marques and A. Costa, "Service life of RC structures: Carbonation induced corrosion. Prescriptive vs. performance-based methodologies," *Construction and Building Materials*, vol. 24, pp. 258–265, Mar. 2010.

[9] T. T. Nguyen, B. Bary, and T. De Larrard, "Coupled carbonation-rust formation-damage modeling and simulation of steel corrosion in 3D mesoscale reinforced concrete," *Cement and Concrete Research*, vol. 74, pp. 95–107, Aug. 2015. Publisher: Elsevier Ltd.

[10] C. Cao, "3D simulation of localized steel corrosion in chloride contaminated reinforced concrete," *Construction and Building Materials*, vol. 72, pp. 434–443, Dec. 2014. Publisher: Elsevier Ltd.

[11] E. Samson and J. Marchand, "Modeling the transport of ions in unsaturated cement-based materials," *Computers & Structures*, vol. 85, pp. 1740–1756, Dec. 2007.

[12] Y. Chen, D. Vasiukov, L. Gélébart, and C. H. Park, "A FFT solver for variational phase-field modeling of brittle fracture," *Computer Methods in Applied Mechanics and Engineering*, vol. 349, pp. 167–190, June 2019.

[13] J. Zhu, R. Zhang, Y. Zhang, and F. He, "The fractal characteristics of

pore size distribution in cement-based materials and its effect on gas permeability," *Scientific Reports*, vol. 9, p. 17191, Nov. 2019. Bandiera_abtest: a Cc_license_type: cc_by Cg_type: Nature Research Journals Number: 1 Primary_atype: Research Publisher: Nature Publishing Group Subject_term: Civil engineering;Composites Subject_term_id: civil-engineering;composites.

[14] Y. Gao, J. Jiang, G. De Schutter, G. Ye, and W. Sun, "Fractal and multifractal analysis on pore structure in cement paste," *Construction and Building Materials*, vol. 69, pp. 253–261, Oct. 2014.

[15] G. Pia and U. Sanna, "A geometrical fractal model for the porosity and thermal conductivity of insulating concrete," *Construction and Building Materials*, vol. 44, pp. 551–556, July 2013.

[16] Q. Zeng, M. Luo, X. Pang, L. Li, and K. Li, "Surface fractal dimension: An indicator to characterize the microstructure of cement-based porous materials," *Applied Surface Science*, vol. 282, pp. 302–307, Oct. 2013.

[17] X. Yang, F. Wang, X. Yang, and Q. Zhou, "Fractal dimension in concrete and implementation for meso-simulation," *Construction and Building Materials*, vol. 143, pp. 464–472, July 2017.

[18] J. Jilesen, J. Kuo, and F.-S. Lien, "Three-dimensional midpoint displacement algorithm for the generation of fractal porous media," *Computers & Geosciences*, vol. 46, pp. 164–173, Sept. 2012.

[19] B. Zhang and S. Li, "Determination of the Surface Fractal Dimension for Porous Media by Mercury Porosimetry," *Industrial & Engineering Chemistry Research*, vol. 34, pp. 1383–1386, Apr. 1995. Publisher: American Chemical Society.

[20] D. Winslow, J. M. Bukowski, and J. F. Young, "The fractal arrangement of hydrated cement paste," *Cement and Concrete Research*, vol. 25, pp. 147–156, Jan. 1995.

[21] S. Torquato, *Random Heterogeneous Materials*, vol. 16 of *Interdisciplinary Applied Mathematics*. New York, NY: Springer New York, 2002.